CHAPTER 9

Source identification and apportionment

An attempt has been made to calculate the contribution of activities in mining industry in degrading the quality of air. Various existing models and techniques used are discussed in this chapter.

9.1 Introduction

It is a matter of the fact that air pollution causes adverse effects on the natural environment. In India, amongst all of the available fossil fuels, India's most significant benefit is coal, and it has shown excellent development in the last two decades **[152]**. Currently, ~90% of total coal production in India succeeds in opencast mines **[229]**. However, due to the opium method for coal production, large quantities of water are required due to land mining and poor land, human rehabilitation, resulting in air pollution and global warming **[5,16,82]**. In many inorganic compounds, the most important are trace metals, which can be emitted by various natural and anthropogenic sources such as crustaceous materials, road dust, construction activities, automobiles, coal and oil combustion, incineration and other industrial activities **[12,189,190]**.

Evaluation of pollution in this area is essential because the air quality has a significant impact on the workers of the mine and the residents living around the city. The primary pollution sources in the study area are due to many harmful gases and an increase in the emissions of traffic from opencast mines, coal–based industries, and diesel–based vehicles, releasing pollutants in the air in large quantities, coal gorges and the growing population of heavy and light–duty vehicles). The introduction of new mining technology, which provided new machinery and technology to coal mining areas, also increases pollution

[230]. The monitoring of ambient air quality is the first step to check the pollution status in the area. Overall, this study illustrates a systematic investigation of the identity and deformation of sources in the study area.

9.2 Receptor modeling for source identification and apportionment

9.2.1 X–ray diffraction of deposited particles

Identifying the mineral in different particulate matter sizes ($PM_{2.5}$, PM_{10}, and SPM) was performed using X–ray diffraction. In XRD, significant peaks were observed between 20 and 70 (2θ), as shown in **Figs. 9.1 & 9.2** of industrial–cum–residential and mining areas, respectively.

The mineral of particulate matter identified in the atmosphere of study area is mainly compound of aluminium silicate (Al_2SiO_5), silicon dioxide (SiO_2), aluminium oxide (Al_2O_3), ferric oxide (Fe_2O_3), Calcium oxide (CaO), ammonium sulphate ($(NH_4)_2SO_4$), potassium chloride (KCl), potassium oxide (K_2O) and others. It may provide an active profile of the reflection plane at that peak position. The intensity of all other reflections from all other compounds is fragile.

A higher value of intensity in the diffractogram indicates the more excellent reflection of incident X–rays by atoms in the identified compound plane. It has been observed that Al_2SiO_5, Fe_2O_3, $(NH_4)_2SO_4$ and KCl compounds are commonly found throughout the study area, indicating the possibility of coal combustion, mining and its associated activities nearby the study area **[231,232]**.

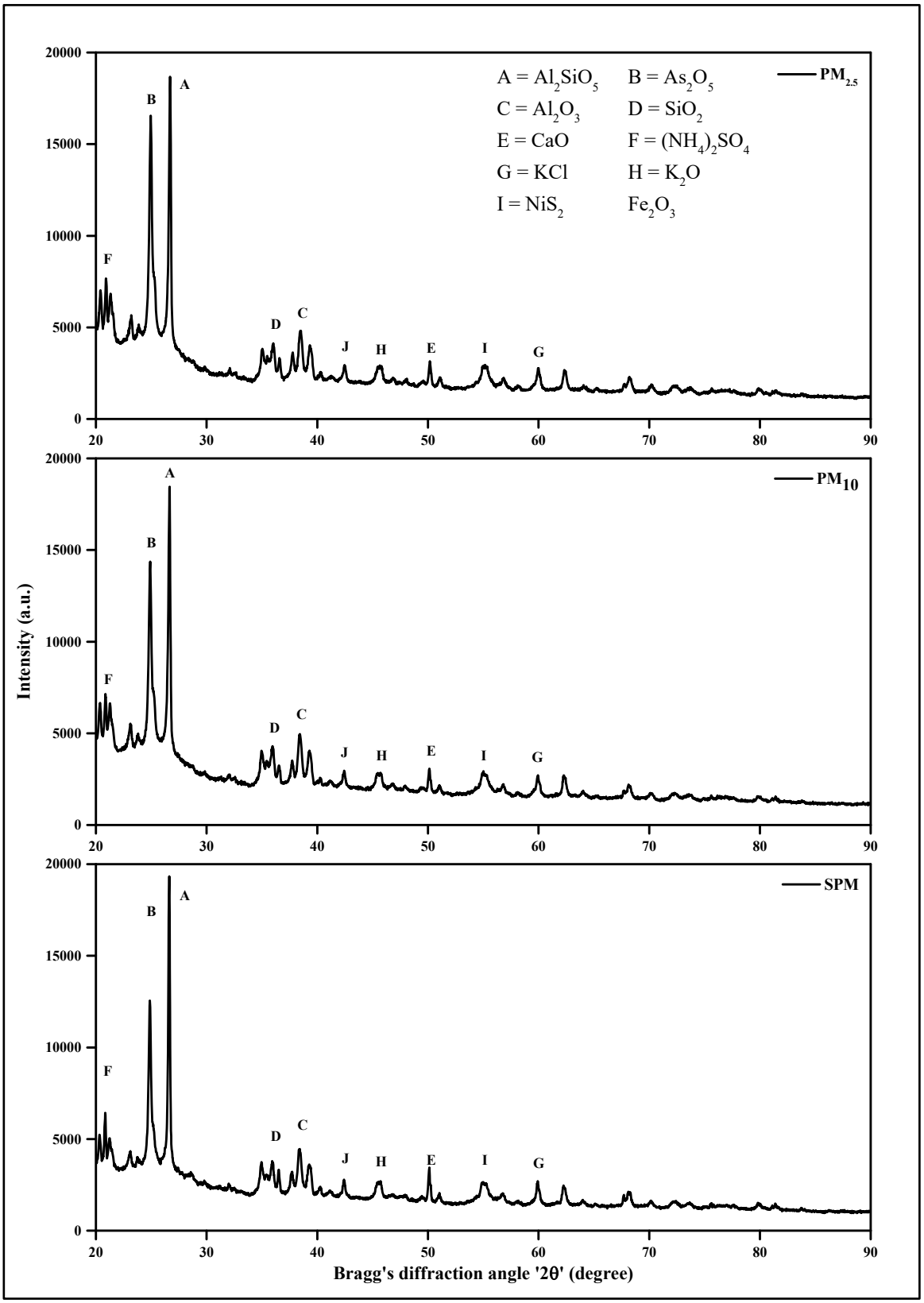

Fig. 9.1: X–ray diffraction patterns of different size particulate matter at industrial–cum–residential area of the study area

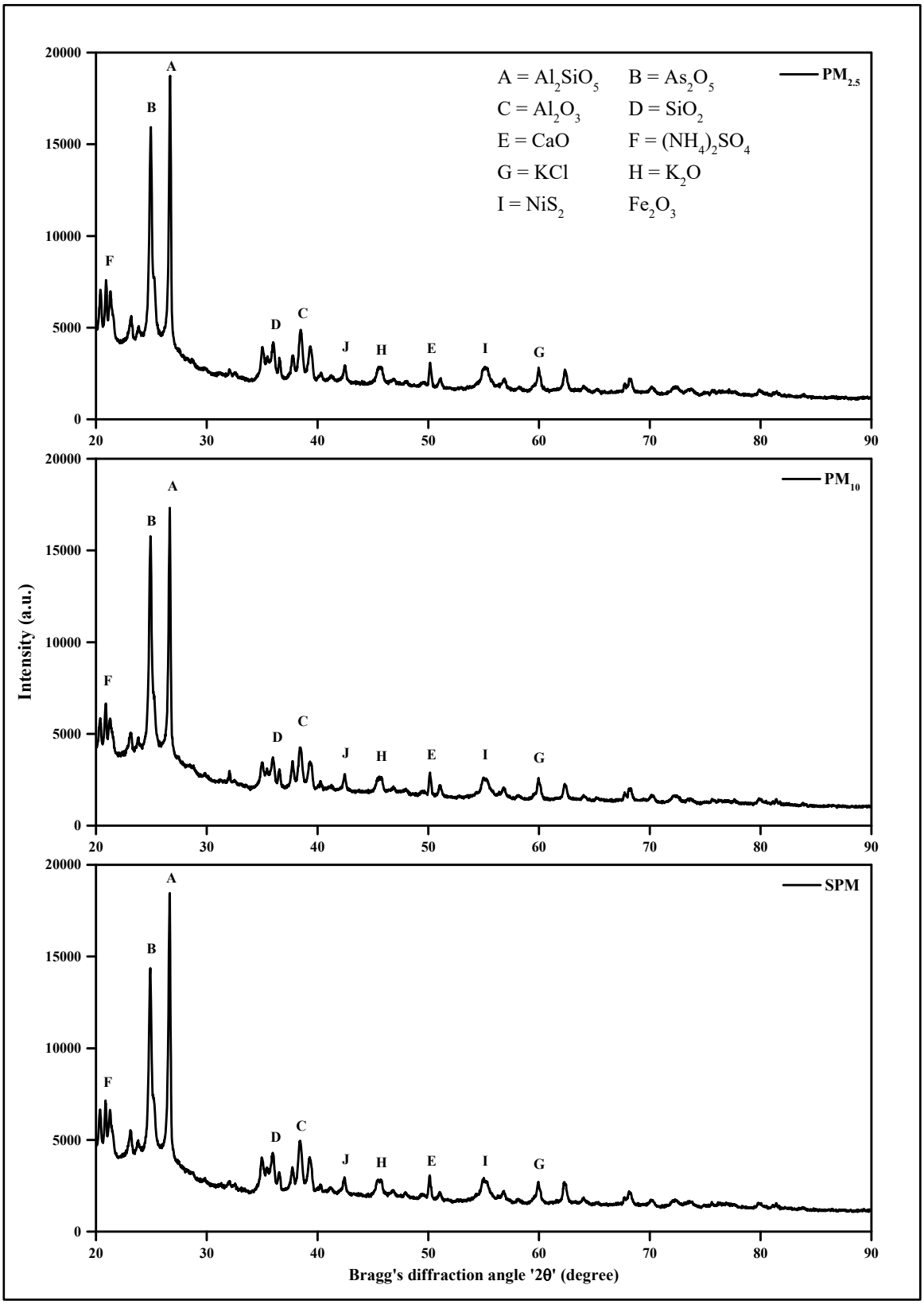

Fig. 9.2: X–ray diffraction patterns of different size particulate matter at mining area of the study area

However, the compounds of Al_2SiO_5, Al_2O_3, As_2O_5, SiO_2, Fe_2O_3, CaO, $(NH_4)_2SO_4$, NiS_2, KCl, and K_2O were found to be present at both the study area. Al, Si, and Fe were observed mainly due to coal combustion, resuspended road dust, crust emissions, and probable source of compounds NiS_2 and As_2O_5 were traffic–related emissions. In the mining area, compound Fe_2O_3, and KCl, $(NH_4)_2SO_4$ were supposed to generate from crust emission and mining activity. Also, oxides and sulphates are produced to open biomass burning and mine activities along with traffic–related emissions. In this area, compounds Al_2SiO_5, As_2O_5, SiO_2, Fe_2O_3, NiS_2, KCl, and K_2O indicated the combined effects of open biomass burning traffic–related emissions along with emission dust from thermal power plants are the major exploiter of the study area. Sulphate is mainly coming from coal–burning **[231]**, and the experimental patterns were compared with patterns obtained from the JCPDS database **[233]**.

9.2.2 Morphology of deposited particles

Morphology and chemical composition in the particulate matter can help to identify these particulate matter sources. Microphotographs of the different size particulate matter collected on the filters and shown in **Figs. 9.3 to 9.5,** along with their sizes. From **Figs. 9.3 to 9.5**, it may be inferred that the particulate matters are showing in shape and type of cubes, rectangle, rough rectangle, and spherical and agglomerates types.

In general, according to morphology, it can be divided into two categories; particles of natural origin (soil dust or minerals) and anthropogenic origin (e.g., from combustion processes). Natural sources' morphology is stable and has irregular shapes **[234]**, mostly dependent on mineral habits, composition, lifetime, and transportation. Particles produced from the combustion processes are solid and liquid particles with variable morphologies; in general, particles with spherical shape result from the secondary reactions **[234],** while

irregular particles in the excellent range result in coagulation processes **[235]**. This type of particles occurs as an individual particle and aggregated form numerously in the current study.

Micrographs also clearly show some irregularly shaped particles. These particles are mixed in composition and are assumed to result from chemical reactions between pre–existing particles, liquid, or gaseous phase. Li and Shao **[236]** have also suggested that alkaline mineral particles react with gaseous species (such as SO_2, NO_2, and HNO_3) and form the coating on the pre–existing particles of minerals.

In this study, the scanning electron microscope microphotograph of particulate matter collected showed that most of the particles possess rectangle and rough rectangle structures. The EDS analyses also show that the particulate matter samples' dominant mineral phase is silica and a trace amount of Al, Fe, and Si. The spherical particle shown in **Figs. 9.3 to 9.5** could be from fly ash origin **[90]**.

These particles can be related to coal combustion from industrial areas and biomass burning, and natural dust **[231,234]**. As far as the elemental composition is concerned, Si is dominant in both the aerosol phase, followed by the other elements. The source may be from traffic–related emissions or other anthropogenic activities. In both study areas, large–sized crystal types of particulates were observed (due to mining activities) along with some fine particulates (due to vehicular movement). Further, small irregular particulate matter deposition was analyzed to soil erosion and ash (due to biomass burning).

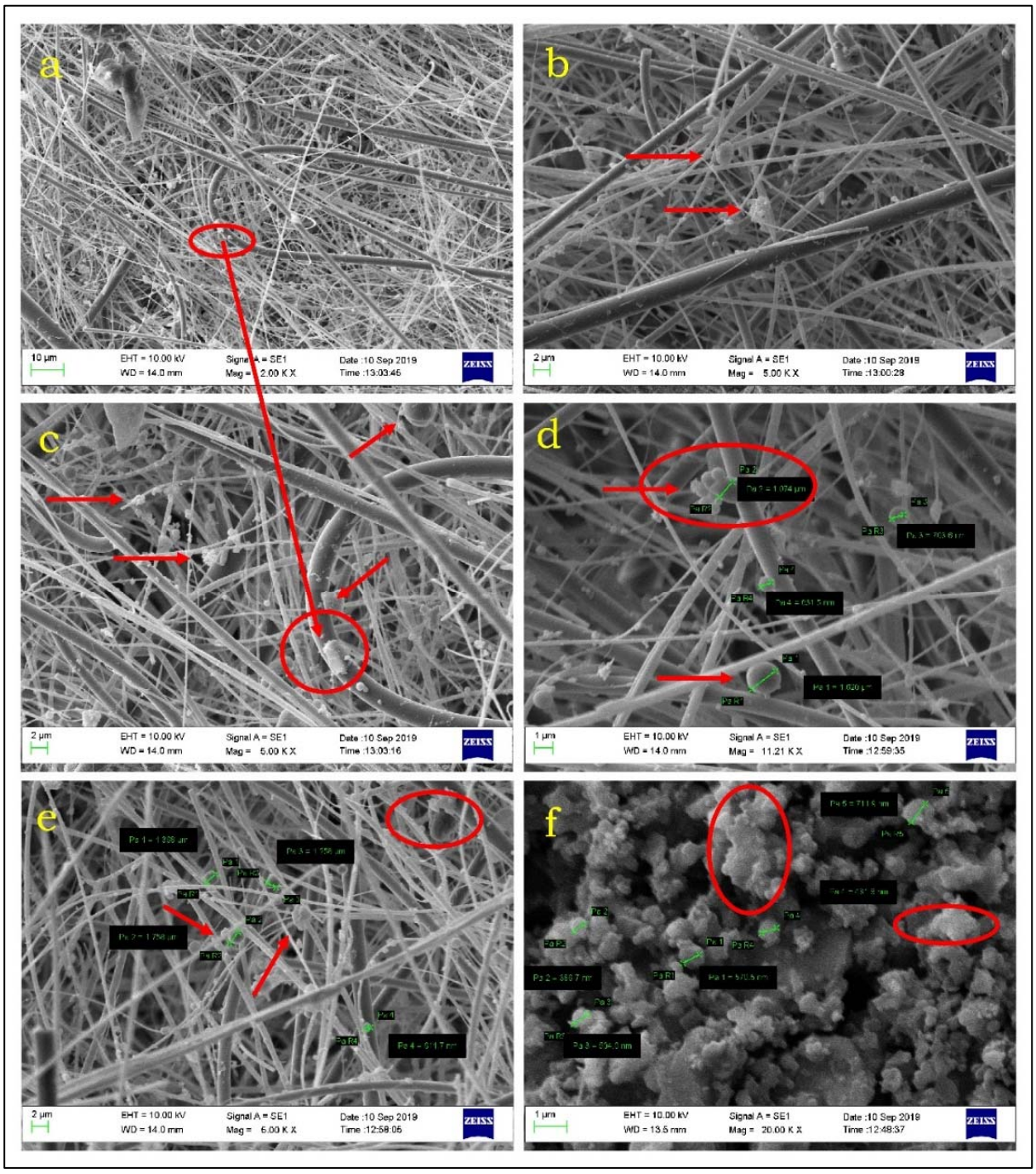

Fig. 9.3: Scanning electron micrograph of particles according to morphological similarities, i.e. soot particles; spherical particles; biological particles; natural and anthropogenic silicate particles and stick–shaped in $PM_{2.5}$ collected in PTFE at study area; **a)** different particles deposited on filter paper; **b)** twinned crystal aggregates of silicate (EDS, Si, Al, Hg, C, S); **c)** capsule shape along with soot particles; **d)** aluminosilicate (EDS: Si, Al, O; size: 1.62 µm); e) capsule shape along with soot particles (EDS: S, Fe, Cu; size 1.75 µm); **f)** smooth surface (EDS: Al, Si, C, Fe; size: 570 nm)

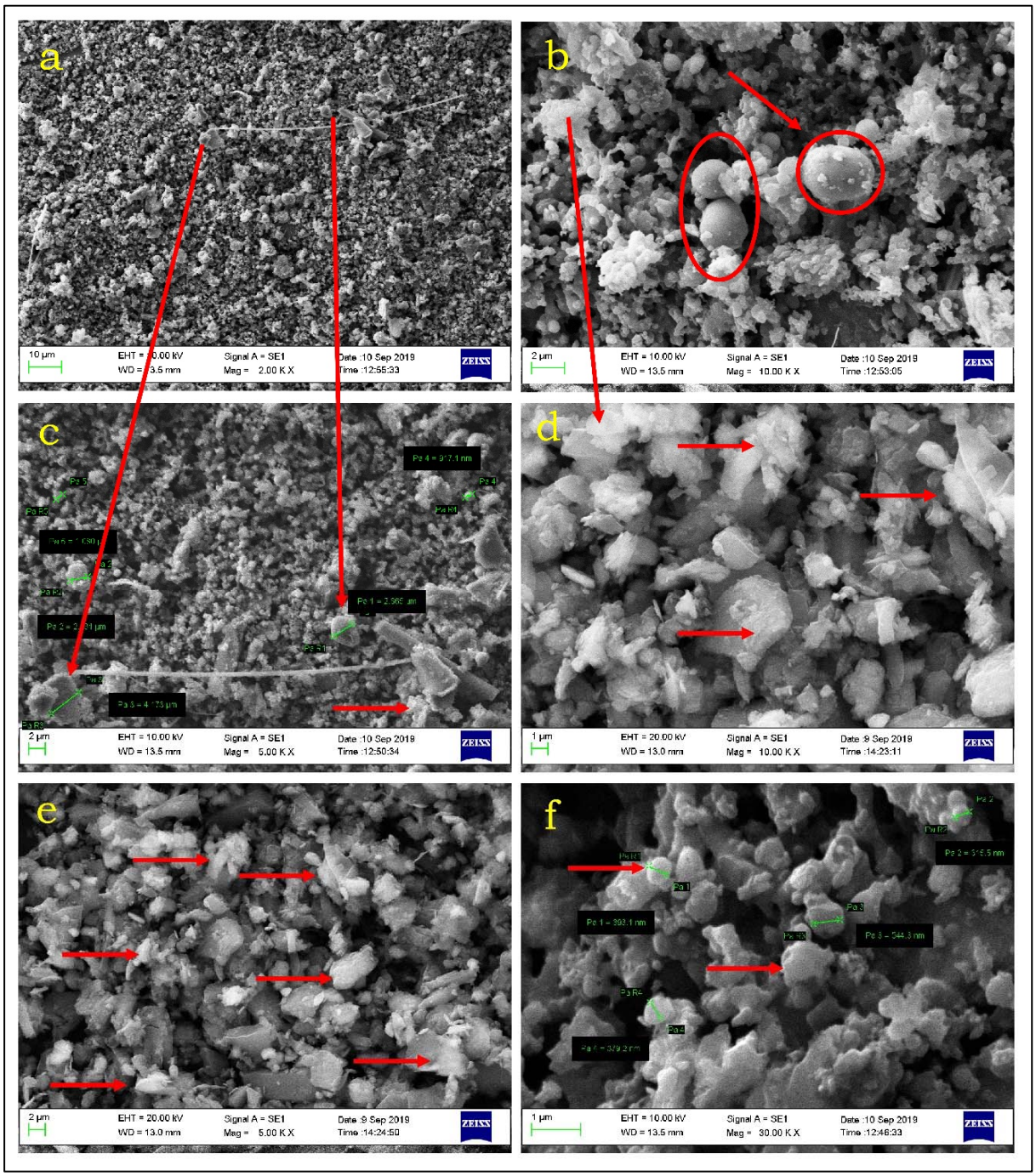

Fig. 9.4: Scanning electron micrograph of particles according to morphological similarities, i.e. soot particles; spherical particles; biological particles; natural and anthropogenic silicate particles and stick–shaped in PM_{10} collected in glass fiber at study area; **a)** different particles deposited on filter paper; **b)** soot particles; spherical particles; **c, e, & f)** natural and anthropogenic silicate particles and stick–shaped (EDS: Al, Si, Cl, S, C; size 3.26 µm); **d)** rough spherical (EDS: Si, Al, Ca, S)

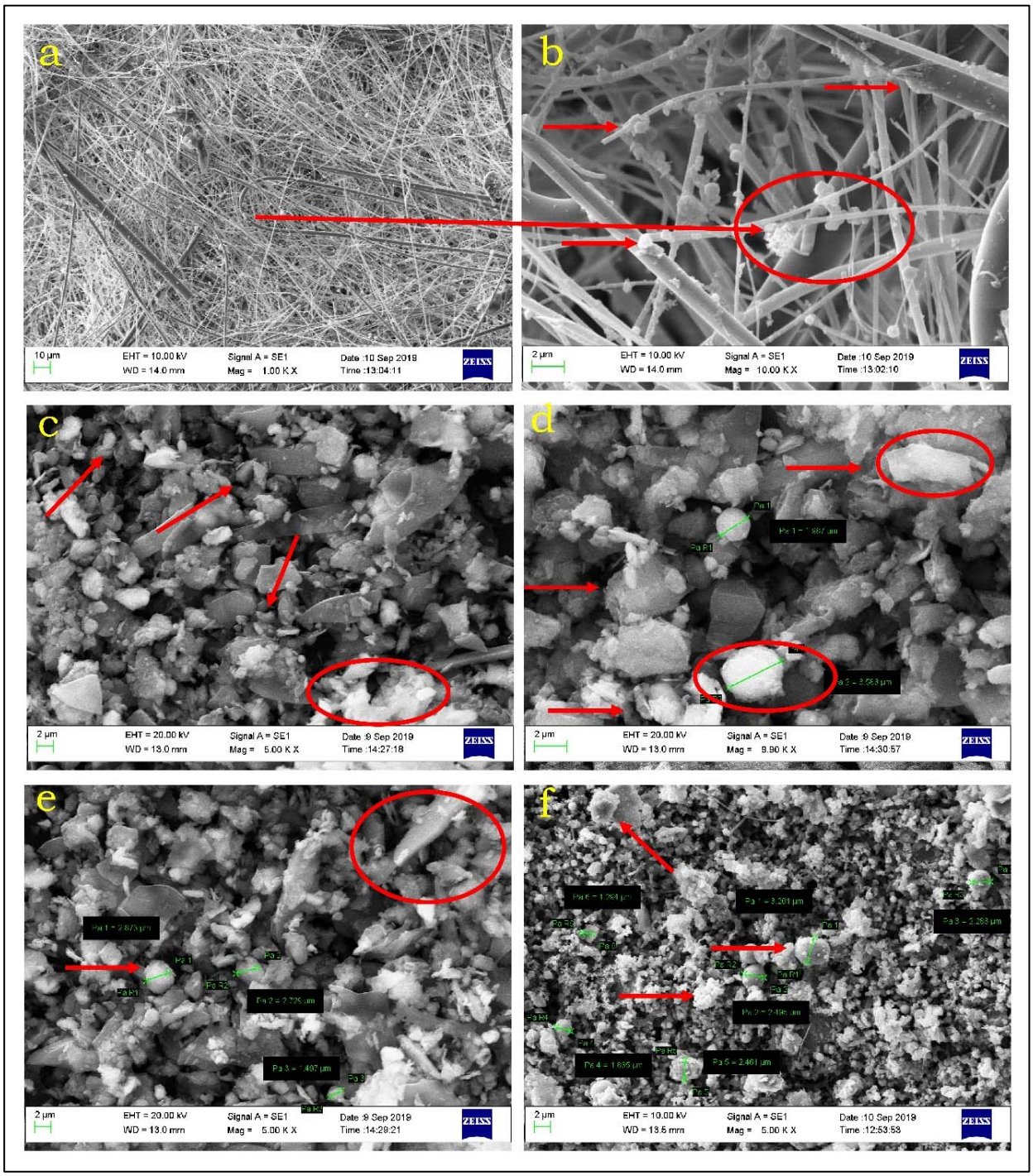

Fig. 9.5: Scanning electron micrograph of particles according to morphological similarities, i.e. soot particles; spherical particles; biological particles; natural and anthropogenic silicate particles and stick–shaped in SPM collected in glass fiber at study area; **a**) different particles deposited on filter paper; **b)** rod shape (EDS: Ca, C, O); **c)** rough spherical (EDS: Si, Al, Ca, S); **d, e, & f)** soot particles; spherical particles; natural and anthropogenic silicate particles (EDS: Al, Si, Cl, S, C; size 3.26 µm)

9.2.3 Principal component analysis

The application of principal component analysis on forty–three air quality parameters resulted in five major factors contributing to around 85% of the total variance in $PM_{2.5}$, PM_{10}, and SPM for the Singrauli coalfield area **(Tables 9.1, 9.2, and 9.3)**. The study is having a similar nature of the loading of pollutants on different parameters. The environmental conditions are nearly the same in both the industrial–cum–residential area and mining area. The study area is surrounded by thermal power plants and opencast coal mines. The variables with close associations were different components grouped; each component indicates one source type and metals associated with that source. There is a chance that one element may represent the mixing of more than one source of similar intensity/impact. The varimax rotated factor analysis identified five possible factors (based on factor loading of species greater than 0.6), indicating five different contributing sources for the species measured in study areas. The principal component analysis results in the study area have been presented **(Tables 9.1, 9.2, and 9.3),** with their different particulate matter size, i.e., $PM_{2.5}$, PM_{10}, and SPM. Thus, the representative basis of analyzed elements has 89.47 and 81.97%, 90.18 and 84.13, and 91.77 and 87.43%, in industrial–cum–residential area and mining area with different size of particulate matter i.e., $PM_{2.5}$, PM_{10}, and SPM, respectively, of the total variance of the data set, as described in the following.

The first factor corresponding to the maximum Eigenvalue (4.13) and (3.86) accounted for 28% and 30% of the total variance associated with $PM_{2.5}$ in Industrial–cum–residential and mining areas, respectively. For 1st factor, As, Cl^- , and SO_4^{2-} had the highest factor loading values (>0.80) in both study areas, which indicated that these were the most influential parameter of the first factor or component. Positive loading of Al, Cr, K, Mg, Ni, Se, Si, Sr, NO_3^-, NH_4^+, NO_2, and SO_2 in $PM_{2.5}$ in Industrial–cum–residential area indicates that this factor may be associated with the coal combustion residue, burning of coal, mining

activity **[237,238]**. Similar to the positive loading of Al, Cr, Se, Si, Cl^-, and NO_3^- in $PM_{2.5}$ in mining areas, this factor may be associated with the coal combustion residue, burning of coal, and mining activity **(Table 9.1) [229,238]**. As and Se, the atmosphere is all associated with burning fossil fuels and coal **[12,239]**. The Cl^- is formed as a by–product of incomplete combustion processes involving carbon–based energy sources, such as the burning of coal or wood. In the vicinity of the Industrial–cum–residential area, residential people use coal as a cooking source. Due to the burning of coal, the NO_2 is observed in this area. Though NH_4^+ is associated with factor 1, these pollutants are not directly related to the burning of coal, and the NH_4^+ in the atmosphere is due to the rearing of cattle and crops **[240]**.

The second factor corresponding to the second eigenvalue (3.48) and (3.12) accounted for 28% and 20% of the variance at Industrial–cum–residential and mining areas, respectively in $PM_{2.5}$, while the third factor with an eigenvalue of (2.86) and (2.34) accounted for 13% and 15% of the total variance at Industrial–cum–residential and mining areas, respectively in $PM_{2.5}$. The last factor (Factor 5) has extracted with eigenvalue (1.05) and (1.09) of accounted for 8% and 7% variance with the high component score for two toxic elements (Cd and Hg). In this factor have positive loading Cu, Pb, and Zn of $PM_{2.5}$, PM_{10}, and SPM at Industrial–cum–residential area and it may be associated with direct traffic–related emission i.e., petrol vehicles, diesel vehicles, fuel oil burning, kerosene generator set **[93,241,242]**.

In the mining area, the second component (Factor 2) was dominated by K, Li, Mg, Mn, K^+, Mg^{2+}, and NO_3^- in $PM_{2.5}$, PM_{10}, and SPM, respectively. These areas may be associated with soil dust, mining activity (i.e., transportation of overburden and coal, drilling, blasting) **[40,238]**.

Table 9.1: Varimax rotated factor loading matrix for the elemental concentrations in $PM_{2.5}$

Parameter	Industrial–Cum–Residential Area					Mining Area				
	1	**2**	**3**	**4**	**5**	**1**	**2**	**3**	**4**	**5**
Ag	0.23	0.25	–0.13	0.12	0.32	–0.12	0.30	0.08	0.09	0.29
Al	**0.76**	0.45	**0.66**	0.01	**0.61**	**0.65**	0.58	0.47	–0.45	0.58
As	**0.93**	0.24	0.03	–0.09	0.02	**0.81**	0.07	0.09	–0.14	0.23
Br	0.21	0.10	0.38	0.12	0.27	0.15	0.04	0.26	0.11	0.07
Ca	0.26	–0.14	0.41	0.23	**0.64**	0.28	0.38	0.17	0.02	**0.68**
Cd	–0.16	**0.72**	0.33	0.03	**0.71**	0.12	0.14	**0.67**	0.18	**0.67**
Co	–0.20	0.13	0.02	0.14	0.13	0.23	0.13	0.18	–0.07	0.19
Cr	**0.78**	**0.74**	0.03	–0.19	**0.68**	**0.71**	0.17	**0.65**	0.16	**0.64**
Cu	0.53	**0.81**	0.22	0.04	0.12	0.28	0.25	**0.60**	0.18	–0.17
Fe	0.26	0.42	0.41	**0.64**	**0.60**	0.43	0.40	0.38	0.56	**0.61**
Hg	**0.82**	0.14	0.15	–0.19	**0.65**	0.49	0.04	0.13	0.10	**0.61**
K	**0.65**	0.18	**0.62**	**0.81**	0.58	0.57	**0.65**	0.12	**0.72**	–0.03
Li	0.22	–0.12	**0.60**	0.01	**0.68**	0.34	**0.68**	0.04	0.02	**0.62**
Mg	**0.80**	0.06	**0.61**	–0.29	–0.03	0.48	**0.63**	0.30	–0.04	–0.02
Mn	0.40	0.28	**0.66**	0.50	0.04	0.47	**0.71**	0.28	0.15	–0.14
Na	0.27	0.12	0.38	0.12	–0.12	0.37	0.28	0.03	–0.16	–0.05
Ni	**0.73**	**0.68**	0.27	**0.81**	–0.15	0.26	0.15	0.60	**0.78**	–0.26
Pb	0.27	**0.95**	0.28	0.07	**0.70**	0.28	0.19	**0.84**	0.24	**0.61**
Se	**0.78**	0.05	0.22	–0.15	0.38	**0.66**	0.31	0.31	–0.03	0.18
Si	**0.77**	0.15	**0.71**	0.03	**0.63**	**0.64**	**0.67**	0.04	0.12	**0.66**
Sr	**0.60**	–0.08	0.59	0.41	–0.06	0.52	0.53	0.40	0.18	–0.04
Th	0.24	0.19	0.09	–0.01	0.19	0.12	0.22	0.13	0.13	0.43
U	0.18	0.04	0.16	–0.05	0.08	0.12	0.14	0.11	0.15	0.24
V	0.14	0.22	0.28	0.04	0.12	0.17	0.11	0.10	–0.18	0.13
Zn	0.45	**0.81**	0.57	–0.41	0.06	0.48	0.40	0.52	0.47	–0.01
C	**0.63**	0.56	0.51	0.04	**0.60**	**0.62**	0.04	0.22	–0.10	**0.63**
H	0.39	0.40	0.10	0.50	–0.06	0.48	0.06	0.28	0.13	0.01
N	**0.63**	0.22	**0.64**	–0.39	0.41	**0.67**	0.19	0.23	0.45	**0.65**
S	**0.61**	0.25	0.25	0.01	0.45	**0.68**	0.22	0.31	0.43	0.26
Br^-	0.09	0.02	0.03	–0.36	–0.36	0.12	–0.10	–0.04	–0.09	–0.24
Cl^-	**0.85**	0.34	0.15	**0.75**	0.19	**0.81**	0.27	0.17	0.49	0.05
F^-	0.45	0.28	0.20	0.18	**0.61**	0.26	0.19	0.10	0.29	**0.62**
NO_2^-	0.57	0.41	0.18	0.19	0.42	0.56	0.13	0.09	0.46	0.39
NO_3^-	**0.66**	0.39	0.16	–0.23	**0.60**	**0.71**	**0.63**	0.23	0.48	**0.65**
PO_4^{3-}	0.08	0.16	0.14	0.03	–0.36	0.13	0.12	0.14	–0.02	–0.36
SO_4^{2-}	**0.87**	0.32	0.45	0.09	**0.62**	0.83	0.13	0.12	0.23	**0.60**
Ca^{2+}	0.22	0.42	0.14	–0.12	**0.71**	0.11	0.19	0.23	0.12	**0.68**
K^+	0.50	0.20	0.56	**0.86**	0.10	0.49	**0.61**	**0.65**	0.46	0.16
Mg^{2+}	0.40	0.03	**0.63**	0.07	0.52	0.15	**0.65**	0.11	**0.65**	0.42
Na^+	0.26	0.04	**0.67**	0.28	**0.63**	0.21	0.12	0.36	0.16	0.59
NH_4^+	0.64	0.43	–0.11	–0.16	0.03	**0.61**	0.16	–0.21	0.40	0.14
NO_2	0.70	**0.69**	0.34	–0.09	**0.61**	0.58	0.22	**0.64**	0.28	0.58
SO_2	**0.68**	**0.74**	0.23	–0.07	0.55	**0.68**	**0.64**	**0.65**	0.23	0.43
Eigen Value	4.13	3.48	2.86	1.76	1.05	3.86	3.12	2.34	1.65	1.09
Percentage of Variance	30.01	28.89	13.21	9.12	8.24	28.95	20.89	15.63	9.16	7.34
Cumulative Percentage	30.01	58.9	72.11	81.23	89.47	28.95	49.84	65.47	74.63	81.97

Note: Factor loading > 0.6; designated on bold type

Table 9.2: Varimax rotated factor loading matrix for the elemental concentrations in PM_{10}

Parameter	Industrial–Cum–Residential Area					Mining Area				
	1	**2**	**3**	**4**	**5**	**1**	**2**	**3**	**4**	**5**
Ag	0.22	0.10	0.03	0.07	0.02	0.18	0.05	–0.07	0.15	0.13
Al	**0.81**	0.41	**0.63**	0.30	**0.64**	**0.75**	**0.60**	0.38	0.20	**0.64**
As	**0.88**	0.21	0.19	–0.11	–0.25	**0.90**	0.09	0.57	0.20	0.40
Br	0.16	0.07	0.35	0.01	–0.23	0.04	0.08	–0.04	0.26	–0.31
Ca	0.27	0.05	0.46	–0.25	**0.69**	0.18	0.44	–0.02	0.46	**0.71**
Cd	0.04	**0.68**	0.46	0.09	**0.68**	0.12	0.26	**0.63**	0.34	**0.63**
Co	0.25	0.04	0.32	–0.02	–0.04	0.13	0.19	–0.02	–0.03	0.03
Cr	**0.71**	**0.71**	0.11	0.20	0.67	**0.75**	0.20	**0.63**	0.05	**0.61**
Cu	0.25	**0.80**	0.06	0.17	0.26	0.29	0.06	0.59	0.08	0.26
Fe	0.16	0.40	0.47	**0.70**	**0.63**	0.17	0.41	0.11	0.67	**0.65**
Hg	**0.76**	0.04	0.21	0.26	0.60	**0.65**	0.17	0.23	–0.34	0.52
K	**0.72**	–0.31	**0.69**	**0.78**	0.49	**0.62**	**0.62**	0.45	**0.69**	–0.13
Li	0.08	–0.13	**0.61**	0.06	0.71	0.11	0.50	0.17	–0.10	**0.73**
Mg	**0.75**	–0.18	**0.63**	–0.07	–0.13	**0.69**	**0.61**	–0.14	0.08	–0.20
Mn	0.32	–0.07	0.58	0.24	–0.32	–0.13	0.49	0.33	0.29	–0.01
Na	0.26	–0.15	0.42	0.23	–0.08	0.22	0.19	0.15	0.29	0.04
Ni	**0.69**	**0.65**	–0.16	**0.75**	–0.42	0.58	0.14	**0.60**	**0.73**	0.02
Pb	0.19	**0.92**	0.30	–0.34	**0.67**	0.16	0.35	**0.86**	0.18	0.58
Se	**0.72**	0.16	0.05	0.24	0.30	**0.78**	0.12	0.26	0.11	0.32
Si	**0.75**	–0.02	**0.68**	0.37	**0.69**	**0.65**	**0.65**	0.08	0.02	**0.72**
Sr	0.58	0.21	0.57	–0.24	0.30	0.52	0.58	0.42	–0.12	–0.13
Th	0.11	–0.03	0.13	–0.04	0.30	0.09	0.11	0.11	0.17	–0.12
U	0.06	0.14	0.06	0.05	0.05	0.03	0.08	0.08	0.04	0.03
V	0.41	0.17	0.15	0.19	–0.11	0.40	0.16	–0.01	0.15	0.01
Zn	0.49	**0.72**	0.51	0.04	–0.23	0.51	0.38	0.58	–0.02	0.04
C	**0.71**	0.58	0.08	0.25	**0.63**	**0.68**	0.57	0.43	0.38	**0.67**
H	0.51	0.42	–0.02	0.14	0.43	0.52	0.07	0.48	0.16	0.16
N	**0.68**	0.31	**0.72**	–0.33	0.19	**0.70**	0.08	0.37	0.04	**0.68**
S	**0.63**	0.28	0.02	0.22	–0.33	**0.69**	0.44	0.21	0.23	0.02
Br^-	–0.09	–0.09	–0.03	0.02	–0.36	0.11	0.07	–0.38	–0.04	–0.08
Cl^-	**0.79**	0.07	0.35	**0.73**	0.58	**0.73**	0.15	0.30	**0.68**	0.54
F^-	0.24	0.17	0.15	0.36	0.14	0.27	0.08	0.12	0.40	0.36
NO_2^-	**0.61**	–0.11	0.11	0.22	0.52	0.58	0.01	0.53	0.17	0.51
NO_3^-	**0.69**	0.14	0.39	–0.10	**0.64**	**0.76**	**0.67**	0.50	0.46	**0.68**
PO_4^{3-}	0.05	0.43	0.11	–0.29	–0.03	0.04	0.02	0.12	–0.41	–0.03
SO_4^{2-}	**0.82**	–0.14	0.04	0.20	0.42	**0.71**	0.30	0.25	–0.09	0.41
Ca^{2+}	0.15	0.04	0.56	0.27	**0.69**	0.17	0.54	0.02	0.30	**0.64**
K^+	0.52	–0.35	**0.61**	**0.81**	0.09	0.50	**0.62**	**0.63**	**0.74**	–0.23
Mg^{2+}	0.38	0.24	**0.63**	0.24	0.10	0.41	**0.68**	0.19	0.44	0.21
Na^+	0.03	–0.06	0.10	–0.13	0.58	0.12	0.44	0.02	0.01	0.54
NH_4^+	0.26	0.04	–0.16	–0.13	0.22	0.14	0.11	0.21	–0.29	0.12
NO_2	**0.81**	**0.70**	0.12	0.07	0.54	0.57	**0.65**	**0.60**	0.15	0.43
SO_2	**0.65**	**0.65**	0.15	0.30	0.43	0.35	0.25	0.58	0.20	0.31
Eigen Value	3.95	3.25	2.5	1.62	1.03	3.72	3.1	2.18	1.6	1.04
Percentage of Variance	31.36	24.64	15.12	10.18	8.88	29.18	21.12	14.16	10.48	9.19
Cumulative Percentage	31.36	56	71.12	81.3	90.18	29.18	50.3	64.46	74.94	84.13

Note: Factor loading > 0.6; designated on bold type

Table 9.3: Varimax rotated factor loading matrix for the elemental concentrations in SPM

Parameter	Industrial–Cum–Residential Area					Mining Area				
	1	**2**	**3**	**4**	**5**	**1**	**2**	**3**	**4**	**5**
Ag	0.16	0.21	0.05	–0.09	0.19	–0.07	0.24	0.19	0.17	–0.01
Al	**0.84**	0.14	**0.63**	0.38	**0.70**	**0.82**	0.44	0.13	–0.19	**0.67**
As	**0.85**	–0.14	0.12	0.10	0.10	**0.73**	0.42	0.49	0.10	0.10
Br	0.38	0.20	0.11	0.08	–0.01	0.10	0.05	0.16	–0.01	0.16
Ca	0.43	–0.22	0.48	0.33	**0.73**	0.22	0.39	–0.20	0.22	**0.76**
Cd	0.11	**0.62**	0.06	–0.03	**0.61**	0.07	0.05	**0.60**	0.02	0.53
Co	0.23	0.05	–0.10	–0.05	–0.25	–0.09	0.23	0.04	–0.25	–0.02
Cr	**0.65**	**0.67**	0.08	0.48	**0.62**	**0.60**	0.10	**0.60**	0.09	**0.60**
Cu	0.28	**0.75**	0.24	0.03	0.48	0.24	–0.05	0.67	0.17	–0.01
Fe	0.16	0.45	0.57	**0.81**	**0.70**	0.07	0.55	0.43	**0.85**	**0.74**
Hg	**0.72**	0.24	0.18	0.19	0.54	**0.61**	–0.01	–0.40	–0.09	0.42
K	**0.85**	0.09	**0.68**	**0.71**	**0.65**	**0.72**	**0.62**	–0.06	**0.63**	–0.14
Li	0.15	0.08	**0.62**	0.05	**0.75**	0.17	0.51	–0.07	0.37	**0.80**
Mg	**0.78**	0.07	**0.68**	–0.41	–0.08	**0.69**	**0.65**	–0.06	–0.09	–0.39
Mn	0.36	0.01	**0.61**	0.28	0.03	0.13	**0.60**	0.00	0.05	0.27
Na	0.41	0.39	0.43	–0.04	0.10	0.45	0.35	–0.40	0.09	0.05
Ni	**0.63**	**0.69**	–0.15	**0.61**	–0.12	0.57	–0.33	**0.64**	0.58	0.27
Pb	0.30	**0.88**	0.34	–0.29	**0.60**	0.11	0.28	**0.72**	0.36	0.52
Se	**0.69**	0.08	0.36	0.21	0.24	**0.66**	0.21	0.08	–0.24	0.25
Si	**0.71**	0.03	**0.65**	–0.24	**0.73**	0.58	**0.60**	0.06	–0.02	**0.77**
Sr	0.53	–0.28	0.55	0.28	–0.07	0.42	0.54	–0.28	–0.05	0.24
Th	0.01	0.04	0.12	–0.20	0.21	0.11	0.02	0.02	0.15	–0.16
U	0.11	0.15	0.03	–0.23	0.10	–0.06	0.14	–0.48	0.11	–0.26
V	0.24	0.25	0.13	0.12	0.11	–0.01	–0.27	–0.23	0.12	0.07
Zn	0.48	**0.65**	0.48	–0.21	–0.01	**0.62**	0.43	**0.62**	–0.02	–0.24
C	**0.76**	**0.63**	–0.16	**0.68**	**0.70**	**0.78**	**0.66**	0.58	**0.70**	**0.74**
H	0.28	0.38	–0.45	–0.13	–0.04	0.26	0.12	0.49	–0.05	–0.08
N	**0.70**	0.49	**0.75**	–0.14	–0.35	**0.73**	0.13	0.51	–0.35	**0.62**
S	**0.64**	0.32	–0.35	0.05	–0.17	**0.70**	–0.12	0.34	–0.17	0.02
Br^-	–0.07	–0.08	–0.08	–0.13	–0.33	0.08	–0.10	–0.06	–0.32	–0.14
Cl^-	**0.76**	0.34	–0.02	**0.69**	0.54	**0.75**	–0.17	0.46	0.61	0.50
F^-	0.24	0.16	0.46	–0.09	0.10	0.45	0.28	0.14	0.08	–0.09
NO_2^-	0.37	0.03	–0.30	0.03	0.39	0.47	0.18	0.26	0.13	0.52
NO_3^-	**0.73**	0.10	–0.35	0.45	**0.65**	**0.82**	**0.78**	0.32	0.38	**0.70**
PO_4^{3-}	–0.09	0.21	–0.01	0.16	0.50	–0.03	–0.02	0.21	0.49	–0.03
SO_4^{2-}	**0.81**	0.36	0.03	0.32	0.26	**0.79**	0.12	0.25	0.28	0.28
Ca^{2+}	0.40	0.01	0.57	0.17	0.77	0.45	0.49	–0.04	0.05	**0.81**
K^+	0.47	0.01	**0.63**	0.77	–0.16	0.36	0.58	**0.60**	**0.67**	0.20
Mg^{2+}	0.32	0.02	**0.61**	0.29	0.09	0.41	0.47	0.03	0.07	–0.58
Na^+	0.13	0.01	0.38	0.27	**0.64**	0.48	0.41	–0.03	0.12	**0.63**
NH_4^+	0.36	–0.15	0.35	–0.04	0.19	0.34	0.19	–0.14	0.19	–0.08
NO_2	**0.69**	**0.71**	0.13	0.28	0.51	0.55	**0.62**	**0.60**	0.08	0.40
SO_2	0.58	**0.60**	0.22	0.39	0.42	0.48	0.25	0.51	0.10	0.25
Eigen Value	3.81	3.08	2.34	1.45	1.01	3.56	3.07	2.17	1.42	1.06
Percentage of Variance	32.95	20.73	16.13	11.13	10.83	30.21	23.65	12.67	11.52	9.38
Cumulative Percentage	32.95	53.68	69.81	80.94	91.77	30.21	53.86	66.53	78.05	87.43

Note: Factor loading > 0.6; designated on bold type

The third factor in the industrial–cum–residential area is the positive loading of K, Li, Mg, Si, Mg^{2+}, and Na^{+} of $PM_{2.5}$, PM_{10}, and SPM. This factor may be associated with resuspended road dust, construction dust and soil dust, mining activity, secondary aerosol, and mobile sources **[119,243]**. In the Mining area, the third factor was dominated by Cu, Pb, and K^{+} in $PM_{2.5}$, PM_{10}, and SPM. These areas may be associated with direct traffic–related emission, i.e., vehicle emission and fuel oil burning **[244-246]**. The fourth factor contributes ~9% with high component scores for Fe, K, Ni, and K^{+} the source was identified as biomass burning, industrial emission in different sizes of particulate matter at both study areas **[40,245,247]**.

The final factor fifth have an equal variance of ~7% with high component scores for Al, Ca, Cd, Cr, Fe, Hg, Li, Pb, Si, F^{-}, NO_3^{-}, SO_4^{2-}, Ca^{+}, and Na^{+} in $PM_{2.5}$, PM_{10}, and SPM, respectively at both the study areas. For Pb and Cr, the source was identified as vehicular emissions, which is in the form of re–suspended road dust; for Al, Fe, Li, and Si, the source is identified as a paved road, construction dust and soil dust, and resuspended road dust **[238,248,249]**. The secondary inorganic aerosol is the fifth source to be called out because of its high contributions to Al, Si, NO_3^{-}, SO_4^{2-}, Ca^{+}, and Na^{+} in particulate matter in different sizes in both study areas. The secondary inorganic aerosol is likely to be caused by the following sources: coal combustion, vehicle exhaust, oil burning, biomass burning, mining activity, waste incineration, and household emission via their precursor gas–to–particle conversion **[245,246,250,251]**. Indeed, secondary inorganic aerosols' formation depends on the concentrations of NO_2, NH_3^{+}, and SO_2, temperature, relative humidity, hydroxide/radiation, and night-time chemistry via NO_3^{-} **[250]**.

However, the sources of pollution in both areas are the same, and that it may be mainly contributed by coal combustion, soil dust, biomass burning, mining activity, and traffic–related emission.

9.2.4 Positive matrix factorization

An application of PMF5.0 to the particulate matters ($PM_{2.5}$, PM_{10}, and SPM) data resolved six factors for industrial–cum–residential and mining areas of the Singrauli Coalfield. The mass fraction distribution of species was used to identify the sources were coal combustion, traffic–related emission, resuspended road and soil dust, secondary inorganic aerosol, biomass burning for different sizes of particulate matter mass. Using PMF analysis, we could identify source profiles of particulate matter mass concentrations and source contributions for levels are shown in **Figs. 9.6 to 9.11** in both study areas, respectively.

In the first factor, the higher concentrations of Al, As, C, Cl^-, Cr, Hg, K, Mg, N, Ni, NO_2, NO_2^-, NO_3^-, S, Se, Si, SO_2, and SO_4^{2-} at the study area (Industrial–cum–residential area) in particulate matter samples indicate the significant source of coal combustion and mining activity of $PM_{2.5}$, PM_{10}, and SPM mass. Al, As, Hg, Si, and SO_4^{2-} are known to occur at high temperatures during the combustion of coal and so on. Ni and V are widely used as markers for the burning of heating fuel **[252]**, while Se and Zn are representative marker species for oil–fired power plants and coal combustion, respectively **[253]**. Positive Matrix Factorization analysis shows that coal combustion and mining activity have been contributed ~23% for different sizes of particulate matter mass in both present studies. In other researchers' studies, the critical marker for coal combustion includes As, Se, Te, and SO_4^{2-} , and it has been contributed between 6% and 30% to PM in different studies **[254,255]**.

In Delhi, where three coal–fired thermal power plants are situated within the city boundaries, Sharma et al. **[256]** attributed ~17% of variance as per positive matrix factorization results of coal combustion, while Srivastava and Jain **[257]** attributed ~15% of the difference of $PM_{0.7}$ fraction of the source. Similar sources were found in the other study area (Mining area) **(Figs. 9.9 to 9.11)**.

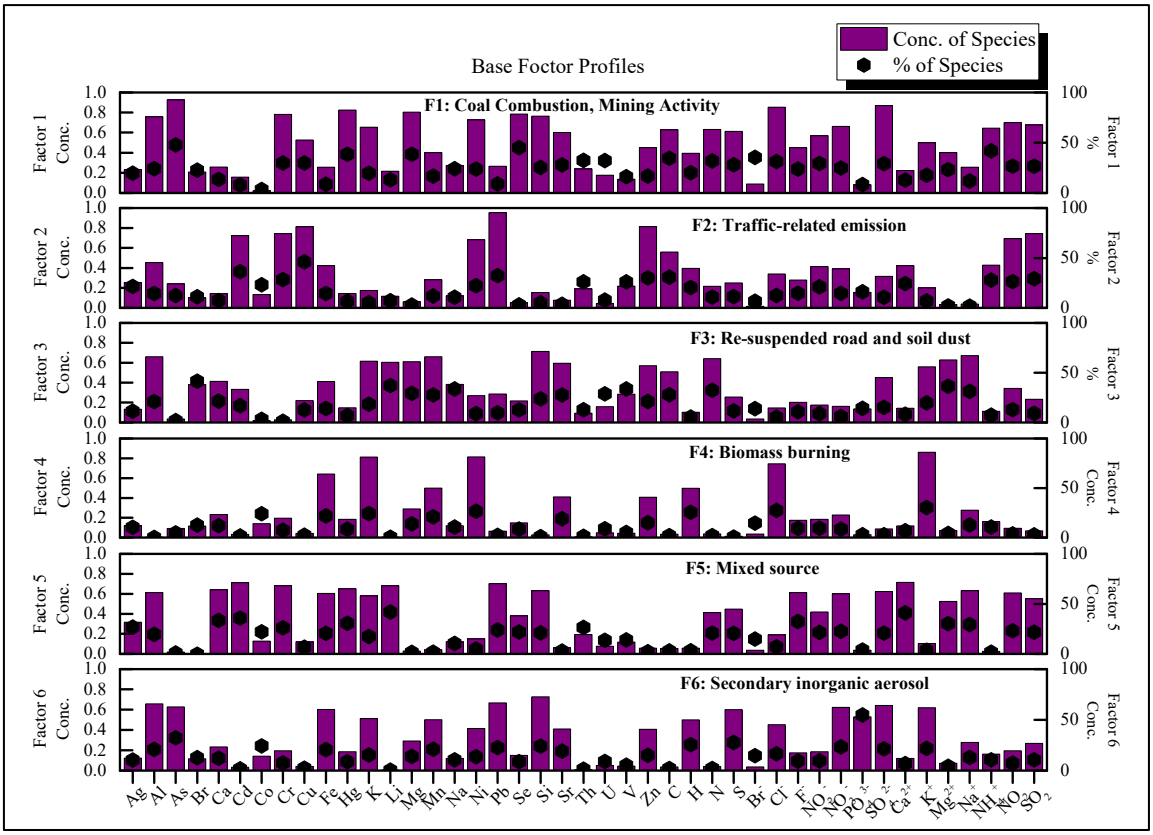

Fig. 9.6: Source profiles of $PM_{2.5}$ aerosol for industrial–cum–residential area

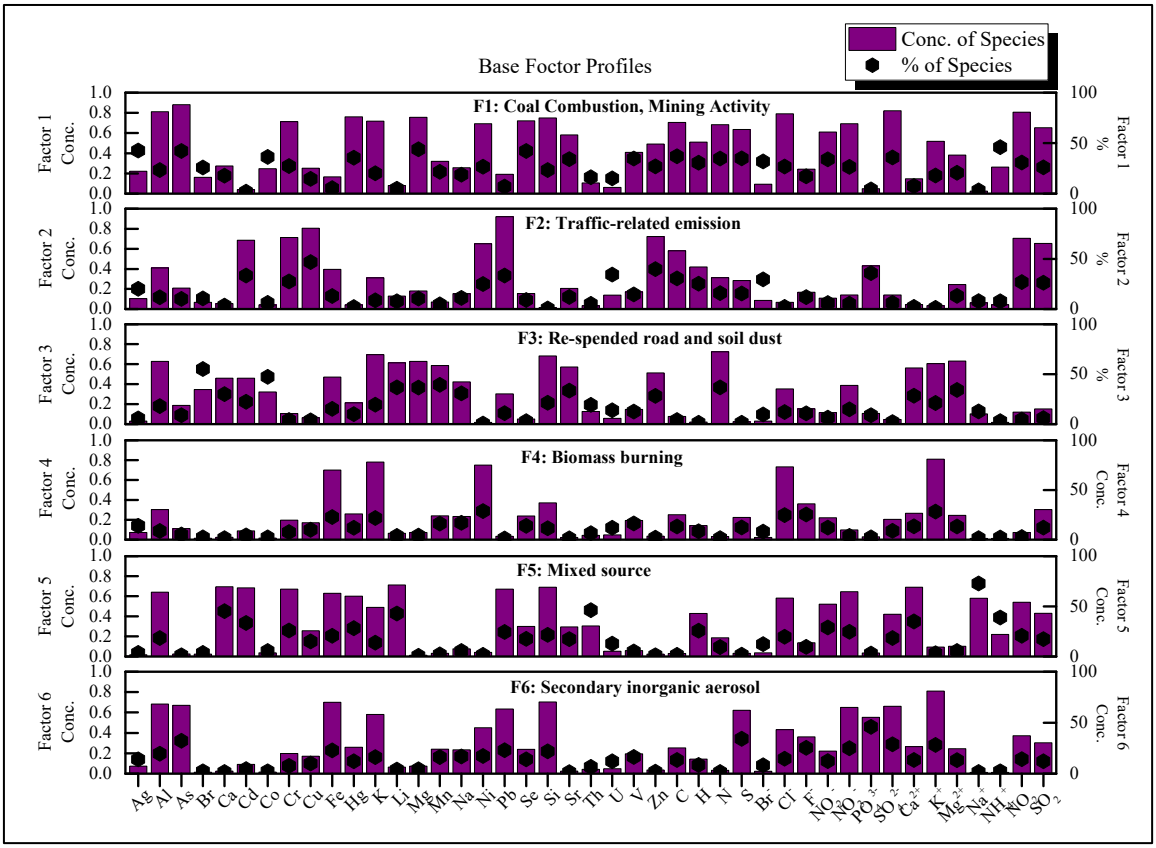

Fig. 9.7: Source profiles of PM_{10} aerosol for industrial–cum–residential area

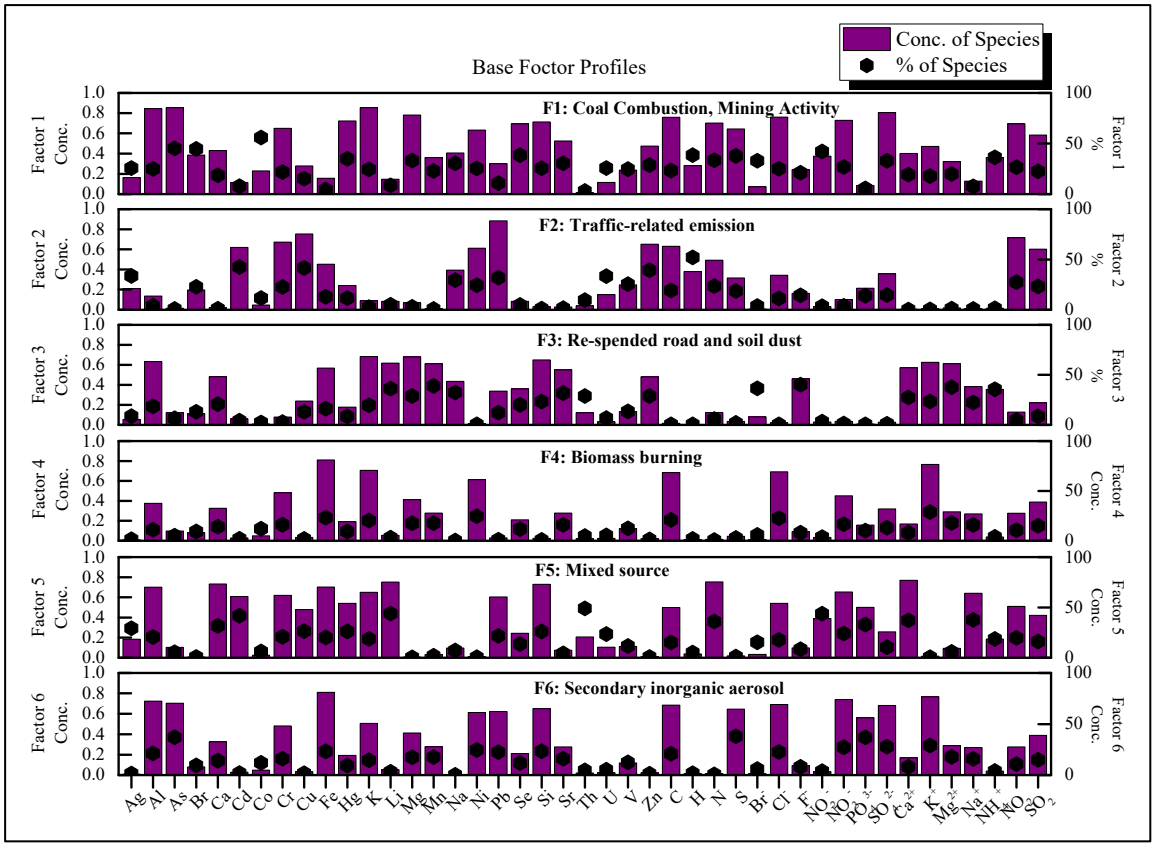

Fig. 9.8: Source profiles of SPM aerosol for industrial–cum–residential area

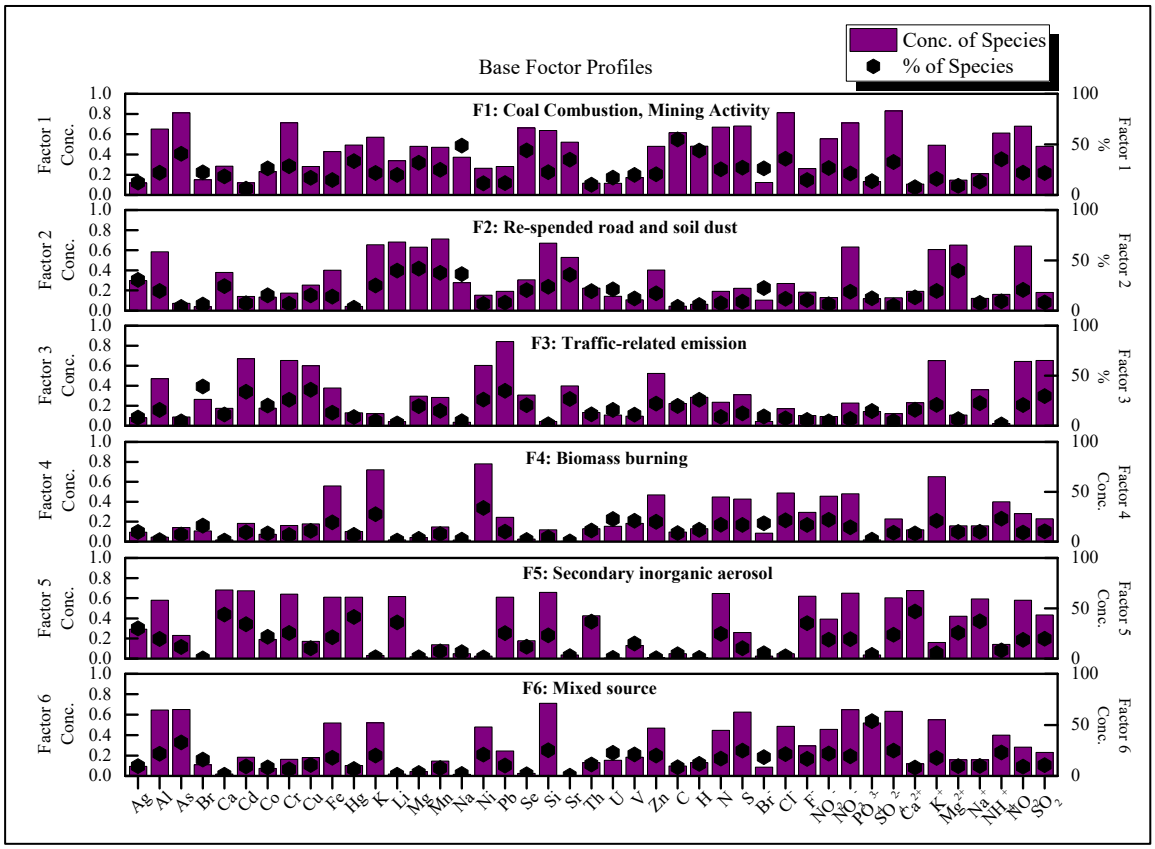

Fig. 9.9: Source profiles of $PM_{2.5}$ aerosol for mining area

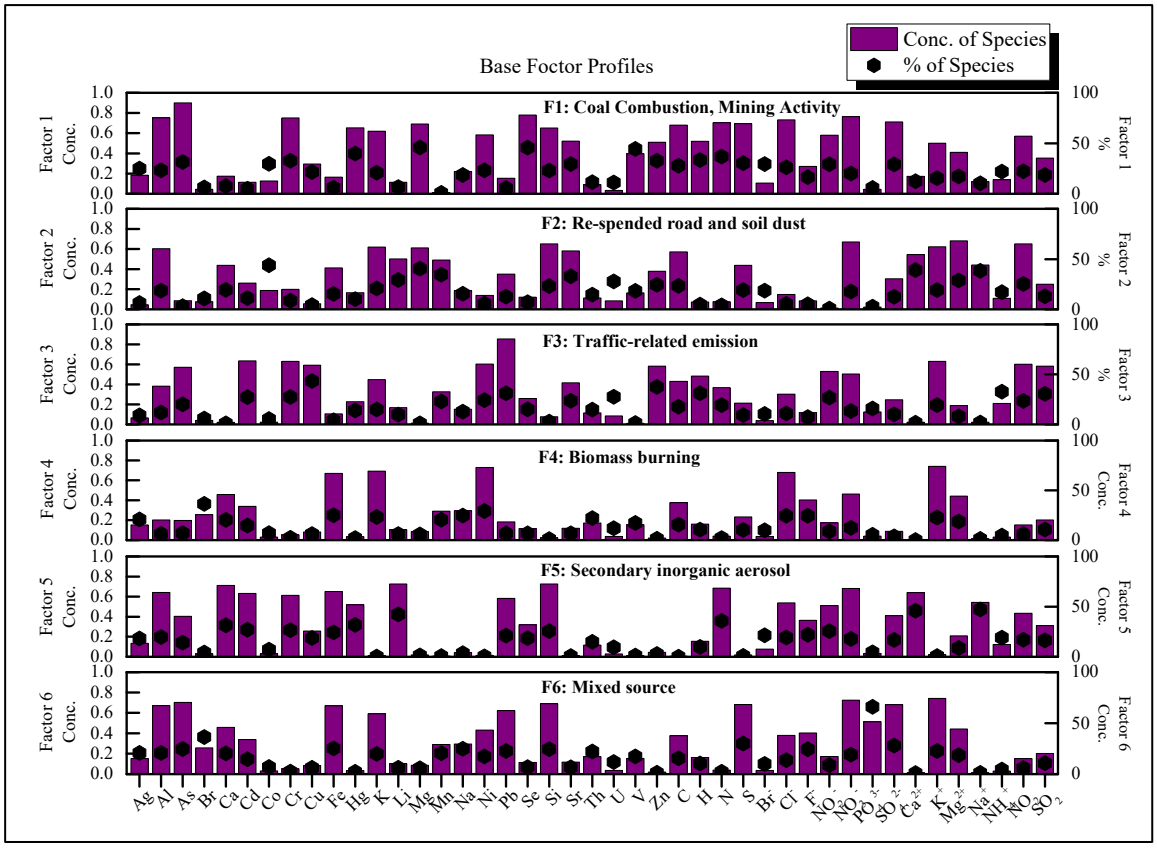

Fig. 9.10: Source profiles of PM_{10} aerosol for mining area

Fig. 9.11: Source profiles of SPM aerosol for mining area

The second source (Factor 2); a vehicle exhaust, is generally dominated by elemental carbon, Cu, Zn, Ba, Sb, Pb, Mn, Mo, and Ni and widely and widely used as markers of traffic–related emission. In the present study (Industrial–cum–residential area), elemental carbon, Cu, Ni, Pb, and Zn have been considered an indicator of traffic–related emission vehicle emission. PMF analysis shows that traffic–related emission has been contributed ~15% for different sizes of particulate matter mass at Industrial–cum–residential area. Furusjo et al. **[258]** suggested that vehicular emission is associated with a high concentration of Cu, Zn, and Sb. Cu, Zn, Mn, Sb, Sn, Mo, Ba, and Fe are markers of brake wear and can serve as traffic re–suspension **[93,190]**. Positive matrix factorization analysis indicates that vehicular emission has contributed to 16.8% in PM_{10} mass in Delhi. In India, V, Mn, Co, Pb, and Zn have used tracer elements to identify vehicular emission **[116,259,260]**. Vehicular emissions are a significant source of particulate matter, and research indicates that they contribute between 10% and 80% to particulate matter in cities across India. A comparison of such estimates is difficult because various studies have quantified multiple vehicles' sources (exhaust, re–suspension, friction, etc.). But the mining area, the soil dust includes most of the crustal elements and has a high concentration of Al, K Li, Mg, Mn, Si, K^+, Mg^{2+}, NO_3^-, and NO_2. These elements are significant constituents of airborne soil and resuspended road dust and usually contribute to coarse aerosol **[237,261]**. The concentration of Al, Li, Si, and NO_3^- of the particulate matter is associated with the re–suspension from mining activity or bare soils by regional winds. In the present study (Mining areas), positive matrix factorization analysis showed that resuspended road and soil dust contributed ~16.5% of the aerosol mass in different particulate matter sizes at the study site. Crustal elements typically used as tracers for soil and crust re–suspension include Al, Si, Ca, Mg, Fe, and Na **[71,245,255]**. A whole array of element tracers used in

India for identifying this source type includes Al, Si, Ca, Ti, Fe, Pb, Cu Cr, Ni, Co, and Mg **[190,260,261]**.

The third source (Factor 3) of metal is referred to as soil and resuspended road dust and contributed ~16% for different particulate matter mass sizes at the industrial–cum–residential area. Crustal metals because of the high percentage of contributions on Al, K, Li, Mg, Mn, N, Si, Sr, Mg^{2+}, and Na^{+} as shown in **Figs. 9.6 to 9.8**. Al, Li, Mg, Mn, Si, and Sr have been recognized as the major constituents of airborne soil and resuspended road dust and collectively make an important contribution to coarse aerosol **[189,251,262]**. The Sr with low EF values were identified as natural sources. Because our study sites are close to the thermal power plants and opencast coal mines, one of India's biggest energy capitals, the heavy windblown soil dust from the mining areas likely contributed to these elements throughout the sample collection duration. But in the other study area (Mining area), the third source was contributing by the traffic–related emission and contributed ~15.5% for different sizes of particulate matter mass at the mining area, as shown in the **Figs. 9.9–9.11**. Industrial and biomass burning contributes the fourth source (Factor 4) of elements, biomass–burning and vegetative burning have been characterized as having high concentrations of Fe, K, Ni, K^{+} , and SO_4^{2-} by various source studies **[262-264]**. These sources also could be possibly facilitated by regional sources or long–range transport. Results show that K, Ni, and K^{+} are contributed by industrial and biomass burning and biomass–burning and crop residue burning in different particulate matter sizes. Positive matrix factorization analysis also shows that biomass burning has contributed ~11.5% for particulate matter mass in both study areas. In India, K^{+} has been used as a key marker for biomass/wood combustion for TSP, PM_{10}, and $PM_{2.5}$ **[245,261],** whereas levoglucosan is the key organic marker **[265]**. Biomass burning has been estimated to contribute in the range of 7–20%, depending upon season and location. It has been reported to be one of the

significant sources in Indian cities, particularly in winter, due to biomass combustion **[40,189,230]**.

The fifth source (Factor 5) was classified as mixed sources, as shown in **Figs. 9.6 to 9.11** (coal combustion, mining activity, traffic–related emission, resuspended road and soil dust, and other unknown sources). The results of the PMF analysis show that mixed sources accounted for about ~17.0% of particulate matter mass, and these sources have contributed the high concentrations included Al, Ca, Cd, Cr, Fe, Hg, Li, Pb, Si, Ca^{2+}, F^{-}, Na^{+}, NO_2, NO_3^{-}, and SO_4^{2-} are widely accepted source markers of coal combustion **[242,245,249, 261]**. For instance, one coal–fired power plant using coal might cause the discharge of Al, As, Hg, Se, NO_2, and SO_4^{2-}. However, it is difficult to predict the sources of F^{-} and Na^{+} in this profile.

The final source (Factor 6) has been mainly secondary inorganic aerosols composed of NO_3^{-} and SO_4^{2-} deriving primarily from the gaseous precursors SO_2, NO_2, and NH_4^{+}. Secondary aerosols of particulate matter (NO_3^{-} and SO_4^{2-}) are originally from anthropogenic or natural sources being formed in the atmosphere. The key markers of secondary inorganic aerosols are NO_3^{-} and SO_4^{2-} and NH_4^{+} and were present in particulate matter mass **[189,245,261]**. The higher concentrations of Al, As, Fe, K^{+}, NO_3^{-}, Pb, S, Si, SO_4^{2-}, at both sampling study areas indicate the primary source of secondary inorganic aerosols of different sizes of particulate matter mass. The present positive matrix factorization analysis shows that secondary inorganic aerosols have contributed ~15.5% for different particulate matter mass concentrations.

The results of the positive matrix factorization analysis show that the secondary inorganic aerosols (~15%), coal combustion and mining activity (~23%), traffic–related emission

(~17%), resuspended road and soil dust (~16%), biomass burning (~12%), and mixed emission (17%) are the major sources of different size of particulate matter mass at both observational areas of Singrauli coalfield. Tiwari **[266]** reported that soil dust contributed 27% of PM_{10} mass in Delhi, whereas Khillare **[267]** estimated 22.0% soil dust coarse particles in Delhi. Chelani **[260]** reported that soil dust and traffic–related emission contributed 17% and 23% of PM_{10} mass respectively at Mumbai, whereas soil dust contributed 37.0% of PM_{10} mass at Kolkata **[255]**.

In the present study, soil dust contributes to ~15% of particulate matter mass at other studies in India, which is more or the same as reported previously, whereas the quantifications of different source types were missing in earlier research. Gugamsetty **[268]** used the PMF model and analyzed that the soil dust (34.0%), traffic–related emission (24.9%), secondary aerosol (24.4%), and sea salt (8.4%) are the significant sources of PM_{10} mass at Shinjung Taiwan. More or less similar source types were also reported **[40,190,259,263]**.

The sources' concentration was varying at different locations due to source strength of particulate matter at sampling sites, sampling duration, sampling time, meteorological conditions, number of samples (with sampling intervals) and number of chemical species.

However, from the above comparison, it is clear that the number and type of source factors derived from the positive matrix factorization analysis in this work are similar to those reported in other studies.

9.3 Conclusions

The morphological study using SEM suggested that the particle shape and size differ depending on its sources. Large–sized, irregular–shaped particles and crystalline particles with irregular shapes were found abundantly in the study area, indicating the sources of particulate matter from the mining and transportation activities in the area. Fine particles with a smoky appearance were also observed, indicating particulate matter generated from coal combustion, traffic–related emission, and biomass burning.

The statistical analysis of principal component analysis and positive matrix factorization, a widely used receptor model, quantified five and six source profiles of particulate matter mass at Singrauli coalfield. The using of principal component analysis, the representative basis of analyzed elements has 89.47 and 81.97%, 90.18 and 84.13%, and 91.77 and 87.43%, in the industrial–cum–residential area and mining area, respectively with different size of particulate matter, i.e., $PM_{2.5}$, PM_{10}, and SPM, respectively, of the total variance of the data set.

The principal component analysis result showed that the contribution of the coal combustion (~30%), traffic–related emission (~25%), soil dust (~13%), biomass burning (~9%) and re–suspended road dust (~7%). The remaining percentage (~16%) is unknown sources of the total particulate matter. The major role of coal combustion and traffic–related emission was also supported by statistical analysis of principal component analysis, as the elements extracted in principal components had a major contribution by elements of coal combustion and traffic–related emission.

The positive matrix factorization analysis quantifies the contribution of the secondary inorganic aerosols (~15%), coal combustion and mining activity (~23%), traffic–related emission (~17%), re–suspended road and soil dust (~16%), biomass burning (~12%), and

mixed emission (17%) are the major sources of different size of particulate matter mass at both observational area of Singrauli coalfield.

Overall, it may be concluded that coal combustion, mining activity, and traffic–related emissions can adversely affect the ambient environment or air quality of nearby regions.